We are IntechOpen,
the world's leading publisher of
Open Access books
Built by scientists, for scientists

6,900
Open access books available

186,000
International authors and editors

200M
Downloads

154
Countries delivered to

Our authors are among the

TOP 1%
most cited scientists

12.2%
Contributors from top 500 universities

CLARIVATE ANALYTICS
BOOK CITATION INDEX
INDEXED

WEB OF SCIENCE™

Selection of our books indexed in the Book Citation Index
in Web of Science™ Core Collection (BKCI)

Interested in publishing with us?
Contact book.department@intechopen.com

Numbers displayed above are based on latest data collected.
For more information visit www.intechopen.com

Main Models of Experimental Saccular Aneurysm in Animals

Ivanilson Alves de Oliveira

Additional information is available at the end of the chapter

1. Introduction

Intracranial saccular aneurysms are lesions of the arteries, the etiology of which remains controversial. Some evidence indicates that intracranial saccular aneurysms arise from a congenital deficiency of the smooth muscle of the arterial wall and local hemodynamic disorders particularly in areas of arterial bifurcation [1], [2]. These aneurysms are less commonly due to trauma, tumors, infections, use of drugs, and conditions associated with high arterial flow {e.g., arteriovenous malformations (AVM)} and connective tissue diseases [3-11]. Saccular aneurysms might be single or multiple and are mostly located in the Circle of Willis. These aneurysms are the most frequent cause of spontaneous subarachnoid hemorrhage (SAH) and primarily affect females. Patients become symptomatic after rupture, which usually occurs between ages 40 to 60 years old[12]. Because rupture is associated with high morbidity and mortality rates, appropriate treatment must be performed as soon as possible. The aim of the treatment is to exclude the aneurysm from the circulation to avoid further bleeding, while preserving the parent artery [13, 14]. Currently, two techniques are available for the treatment of saccular aneurysms: 1) microsurgery (developed by Yasargil), which is based on the placement of a metallic clip in the aneurysm neck [15], and 2) endovascular coiling (developed by Guglielmi), which is based on the introduction of platinum microcoils inside the aneurysms that induce thrombosis and thus isolate aneurysms from the circulation[16]. The continuous development of this latter technique has reduced the morbidity and mortality of the treatment of brain aneurysms [17]; however, improvement of models of experimental saccular aneurysms is needed to develop novel embolization techniques and to test new materials.

2. Selection of the animal species

2.1. Concept of experimental animal

The terms "laboratory animal" or "experimental animal" are somewhat inappropriate because in theory, any animal can be used in laboratory experiments. Nevertheless, both terms are frequently used in scientific literature to refer to animals exhibiting (natural or induced) diseases in which the mechanisms are similar to human diseases.

2.2. Types of experimental models with animals

Experimental models with animals are classified as: 1) induced, 2) spontaneous, 3) negative and 4) orphan[18]. In the induced animal models, the investigated condition is induced experimentally, which can be highly advantageous because these models allow for free selection of the animal species, for example, intake of beta-aminopropionitrile combined with arterial hypertension induces intracranial aneurysm formation in rats [19]. Induced animal models are very important in the development of novel surgical procedures, to assess the viability of procedures and their physiological consequences, and in therapeutic assays, for instance, the surgical creation of aneurysms on the lateral wall of the common carotid artery of dogs [20] and pigs [21]. In spontaneous models, the investigated disease occurs naturally, such as with prostatic hypertrophy in dogs and some diseases in animals with genetic mutations. The spontaneous occurrence of intracranial saccular aneurysms in animals is rare. Negative models involve a particular disease that does not develop in a particular species and, thus, these models are ideal to study mechanisms of resistance or a lack of reactivity to a given stimulus. For example, rabbits do not develop gonorrhea and vultures do no exhibit neoplasms. In orphan models, a disease (or condition) that occurs naturally in non-human species is "adopted" when a similar human disease is identified at a later time (e.g., bovine spongiform encephalopathy, which is also known as mad cow disease) [18].

2.3. Principles for animal selection

Experimental animals should only be used when there are limitations to the research with humans. In therapeutic assays, the use of animals is mandatory and constitutes an essential phase of the preclinical testing of embolization devices or materials. In general, small animals are the most frequently used for research purposes; mice, rats, rabbits, and guinea pigs correspond to 90% of scientific studies [22]. Larger animals such as dogs [20], pigs [21], or monkeys [23] are also used for research purposes, albeit less frequently. Such diversity of species that exhibit different characteristics makes it difficult to select a particular species for experimental aneurysm production. Although there are no specific guidelines on how to perform such a selection, three general principles must be considered: 1) the type of animal that will be used, 2) the type of aneurysm one seeks to simulate, and 3) the aims of the study.

Regarding the animal type, researchers should be thoroughly aware of its biological characteristics, behavior, vascular anatomy, and phylogenetic similarity with humans.

Among the biological characteristics, the size and metabolism of the animals exert a direct influence on the selection. Large animals are more difficult to handle and require more complex infrastructure (lodging, feeding, care, anesthesia, and specialized human resources), which increases the cost of research. In addition, size also influences the number of animals used in experiments. Thus, for ethical reasons, studies that use large animals such as dogs and monkeys restrict their number to the bare minimum needed to ensure the validity of the results. A reduced number of animals influences the statistical methods applied to the analysis, because small samples can reduce the statistical power of tests and lead researchers to infer inaccurate conclusions. In addition, the calculation of the minimum number of animals is difficult because unpredictable losses can also occur as a function of the initial training and pilot study.

With regard to metabolism, different animal species also exhibit different patterns of metabolic rate; for instance, the metabolism of rodents is often faster than that of humans. This metabolic power (also known as metabolic body weight) interferes with the effects of drugs on the organism, as well as with its processing, distribution across organic fluids and tissues, and modes of excretion. Thus, the calculation of experimental doses should be performed according to the metabolic weight rather than the absolute body weight of the animals. In surgical studies, different metabolic rates (influenced by factors such as age, gender, diet, and circadian rhythm) interfere with wound healing and regeneration of tissues and organs, thus encouraging researchers to learn the principles of veterinary anesthesia that correspond to the involved animals, the characteristics of the drugs that will be used, and more specifically, the potential interference of medications with the parameters analyzed in the study[18].

In addition to the biological characteristics, researchers must also be familiar with the intracranial and cervical arterial anatomy of each animal species, and the histology, diameters, flow patterns, and anastomoses of the vessels, because these are essential factors in the selection of the aneurysm construction technique.

The phylogenetic similarity between animals and humans is also important in species selection, but it does not suggest that the extrapolation of the results to humans will be reliable. For example, human immunodeficiency virus (HIV) does not induce immunodeficiency in monkeys, and thus, does not represent the ideal animal model to study acquired immunodeficiency syndrome (AIDS). Transgenic animals have been increasingly used in research studies; however, caution is needed because such animals might exhibit unknown disorders that may interfere with the extrapolation of the results to humans[18].

Once the animal model has been selected, the experiment performed, and the data selected, the stage of explaining the phenomena by means of induction begins. This process consists of verifying a particular fact and its adequation to a known general law. This mode of reasoning has inherent odds of error; thus, one must be cautious in the extrapolation of the

results of experiments performed with non-human species to humans. In other words, compounds that might be noxious to a given non-human species might be innocuous or even beneficial to humans. For example, penicillin is lethal for guinea pigs, but is well tolerated and even beneficial for humans. In addition, aspirin is teratogenic in cats, dogs, rats, guinea pigs, mice, and monkeys, but it is innocuous in pregnant women. Thalidomide is teratogenic in human beings and monkeys, but innocuous in rats and other species. Therefore, phylogenetic proximity is not a fully reliable measure of similarity between the physiological phenomena of animals and humans [18].

To reduce the odds of selecting an inappropriate animal model for a given experiment, the *multispecies approach* is recommended. At least two different species including non-rodents must be used in studies employing drugs, whereas the use of more than one animal species is rare in studies of surgical techniques. Accordingly, some animal species have become traditional standard models for specific surgical procedures. However, surgical studies focusing on the physiological features of a disease require more than one animal species, which despite its usefulness, does not ensure the absolute reliability of the extrapolation of the results from animals to humans [18].

Regarding the aneurysm model, a comprehensive awareness of the available models is required, in addition to their construction techniques, advantages and disadvantages, and more specifically, which features of human aneurysms one seeks to simulate, that is, their histological, geometric, physiopathological, and hemodynamic characteristics (e.g., ruptured or not, small, medium-sized, large or giant, with or without thrombus, on the lateral wall or at a bifurcation, high or low hemodynamic tension, etc.).

Finally, the aims of the study are essential in the selection of the animal species and the techniques that will be used in aneurysm construction, e.g., verification of the physiopathological mechanisms, therapeutic assays, creation of novel surgical/endovascular techniques, or training of doctors in these therapeutic modalities. Regarding the latter issue, medical training using animals is justified as training on humans exposes patients to medical error. Thus, practical training using animal models is indispensable for medical education because it contributes to the development of psychomotor skills and enables physicians to safely perform invasive techniques.

2.4. Main animal species used in the construction of experimental saccular aneurysms

Despite all of the considerations above, the selection of the ideal animal species for studies on experimental saccular aneurysms is not yet well established. As spontaneous intracranial aneurysms rarely occur in animals, most studies employ induced models, which have the advantage of allowing for the free selection of species. Animals such as rats[19], rabbits[24], dogs[20], pigs[21], and monkeys[23] have been used in studies on physiopathology [25, 26], hemodynamics[27-31], and the training of surgical[32, 33] and endovascular techniques, in addition to the testing of embolization devices and new materials[21, 34-38]. In studies aimed at developing surgical/endovascular techniques, it is rare that more than one animal

species is used in the same experimental model; therefore, there are no systematic comparative studies seeking to define which is the ideal animal species for the experimental production of intracranial saccular aneurysms. Nevertheless, in recent years, rabbits (*Oryctolagus cuniculus*) have been preferred for these studies because their coagulation system is very similar to that of humans. Rabbits are easy to handle, and the diameters of their extracranial carotid arteries are very similar to those of humans [39-44].

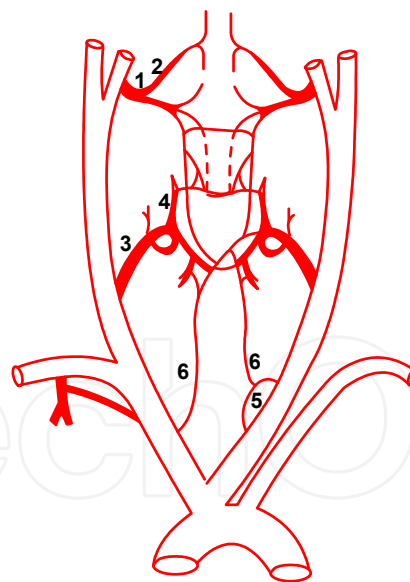## 2.5. Cervicocerebral vascular anatomy of rabbits

Regarding the vascular anatomy of rabbits, knowledge of the cervicocerebral vessels and their connections is essential in the construction of experimental saccular aneurysms. Below, we present a summary of the cervical and intracranial vascular anatomy of rabbits together with their main anastomoses.

The innominate artery (3.5 mm in diameter) is the first branch of the aortic arch, and after running 6 mm, it divides into the right subclavian (2 mm in diameter) and right common carotid (2 mm of diameter) arteries. The left common carotid artery (2 mm in diameter) begins immediately next to or together with the innominate artery. The left subclavian artery (2 mm in diameter) is the last branch of the aortic arch, and it originates from the left vertebral (1 mm in diameter) and superficial cervical (1 mm in diameter) arteries[45]. In the second most frequent distribution type, the aortic arch can only be divided into three branches: the innominate, left common carotid, and left subclavian arteries. Lesser variations might also occur; for instance, the supreme intercostal and left vertebral arteries might originate directly from the aortic arch. The superior thyroid artery usually originates from the common carotid arteries; however, it emerges approximately between the 3rd and 6th tracheal rings and runs towards the thyroid gland, in some cases of only one common carotid artery[46]. Upon arriving at the isthmus, the superior thyroid artery divides into two branches: one ascending (cricothyroid branch) and the other descending (which runs inferiorly between the trachea and the esophagus). The bronchial branches stem from the right supreme intercostal and left common carotid arteries and lead to the tracheoesophageal branches, which run upwards between the trachea and the esophagus and anastomose with the descending branches of the superior thyroid artery[47] (figure 1). These branches rarely exhibit variations, and when they do occur, these variations are more common on the left side[48].

The common carotid artery (CCA) leads to only one branch, namely the thyroid artery, and immediately above it, the CCA divides into the internal and external carotid arteries. The main branches of the external carotid artery (ECA) are the occipital, lingual, external maxillary (facial), and anterior and posterior auricular arteries. Both the auricular and external maxillary arteries emerge separately or from a common trunk. At the level of the zygomatic arch, the ECA divides into the superficial temporal and transverse facial arteries and continues its course up to the pterygoid canal, where it divides into small branches to the posterior side of the orbit and originates the external ophthalmic artery, which in turn forms the lacrimal and frontal branches, and subsequently, the anastomose with the internal
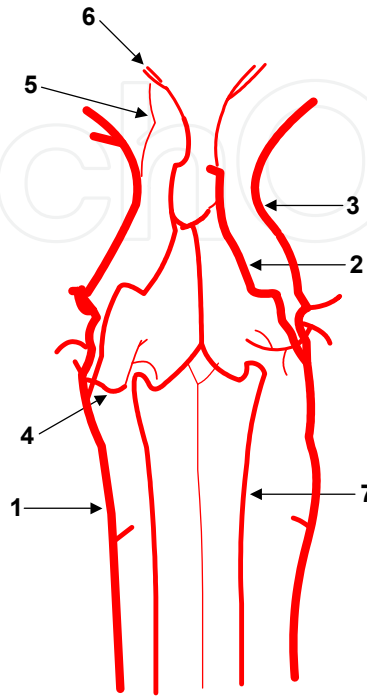
ophthalmic artery. The main branch of the internal maxillary artery is the middle meningeal artery. The intracranial internal carotid artery (ICA) divides into the ophthalmic arteries, cranial, and caudal branches. The cranial branch runs forward towards the uncus, where it divides into the anterior choroidal artery and middle cerebral artery (MCA) trunk, and then continues up to the chiasm, where it unites with the contralateral cranial branch to form a common anterior cerebral artery trunk that separates again at the level of the corpus callosum. The common anterior trunk originates from the lateral artery of the olfactory bulb, which leads to the ethmoidal branches of the cribiform plate. The MCA runs along the lateral cerebral sulcus and divides into the posterior ophthalmic artery, large posterior branch, and large anterior and middle branches, in addition to the small olfactory bulb branches. The caudal branch of the ICA supplies most of the blood flow of the basilar artery (BA) and leads to the following branches: posterior communicating artery, small medial geniculate body branches, large anterior quadrigeminal body, small branches of the posterior side of the uncus, and the posterior segment of the corpus callosum. The cerebellar artery might originate from the ending of the ICA or the BA and connects to several branches of the brainstem. The BA is formed by the fusion of the arteries of the first spinal nerves and divides (on the ventral surface of the trapezoid body) into two vessels that reunite at the upper margin of the pons. In addition, the BA gives small lateral branches, the cerebellar artery and the perforating branches. The arteries of the first spinal nerve then reunite at a lower level and form the ventral spinal artery[49].

Figure 1. Graphic representation of the visceral vascularization of the neck of rabbits. 1- superior laryngeal artery, 2- superior branches, 3- superior thyroid artery, 4- cricothyroid branch, 5- bronchial branch and 6- tracheoesophageal branch. Modified from Bugge, 1967[2].

Regarding the system of intracranial anastomoses in rabbits, the collateral circulation is very different from that of dogs. The internal maxillary artery originates from the orbital branches, which end at the ophthalmic branch and represents an insufficient anastomotic pathway. The anastomotic branches between the orbital and internal carotid arteries are too

small or are absent. A small branch links together the ICA and BA before they unite at the circle. Finally, when an occlusion of the common carotid artery occurs, the supply of blood is provided by the contralateral ICA (**figure 2**)[3].

Figure 2. Graphic representation of the intracranial anastomosis system of rabbits. 1- common carotid artery, 2- internal carotid artery, 3- external carotid artery, 4- occipital artery, 5- orbital artery, 6 – internal ophthalmic artery and 7- vertebral artery. Modified from Chungcharoen, 1954[50].

3. Selection of an experimental saccular aneurysm model

3.1. Concept of experimental saccular aneurysm

Experimental saccular aneurysms are induced aneurysms intended to reproduce the histological, geometric, and hemodynamic characteristics of human intracranial aneurysms.

3.2. Characteristics of an ideal model of experimental saccular aneurysm

With the rise of endovascular treatment of human intracranial aneurysms – by means of embolization using platinum microcoils[16] – experimental models of saccular aneurysm are encouraged to adapt to this novel therapeutic modality by meeting the following criteria: 1) demonstration of long-term permeability in untreated control species, 2) development in animal species with a coagulation system similar to that of humans, 3) simulation of the morphology of arterial bifurcation, terminal artery, or other aneurysmal types that expose the aneurysm neck to high hemodynamic tension, 4) development in vessels with a similar size to human intracranial vessels, 5) development without the need of local surgery to minimize the repair/wound healing response, which might confound the results of the experiment with the natural increase of the biological activity characteristic of several

embolization materials such as: coils, fluid agents, etc., and 6) simulation of the limitations met by embolization of human aneurysms using such materials[39].

3.3. Main models of experimental saccular aneurysm

German and Black (1954) were the first researchers to produce experimental aneurysms using a surgical construction of saccular aneurysms on the common carotid artery of dogs. Such aneurysms mimicked the ones occurring on the lateral wall and were frequently used in hemodynamic studies; however, they produced fibrosis at the suture site, which was a disadvantage[20]. Since then, surgical models have evolved with the culmination of the swine model (1994), consisting of a graft of the venous pouch onto the common carotid artery (CCA) of pigs. This method produces lateral wall aneurysms, but includes disadvantages such as venous histology, induction of intense fibrosis at the suture site, and low hemodynamic tension[16].

In addition to the surgical method, chemical induction might also be used in the construction of saccular aneurysms. The main proponent of this technique was Hashimoto (1970), who induced arterial wall weakening in rats by ingestion of 3-beta-aminopropionitrile, a toxic agent extracted from the seeds of the sweat pea (*Latyrus odoratus*), which destroys the elastic fibers and collagen of the arteries of rats[19]. In addition, Hashimoto ligated one of the common carotid arteries and induced arterial hypertension in rats (via nephrectomy, intake of saline solution, and high doses of corticosteroids) to cause greater hemodynamic tension on the weakened arterial wall[30]. This technique was the first to produce successful intracranial saccular aneurysms at the bifurcations of the cerebral arterial circle. Nonetheless, the aneurysms were too small and were not useful for the development of surgical techniques nor for the study of intra-aneurysmal hemodynamic alterations[26, 29].
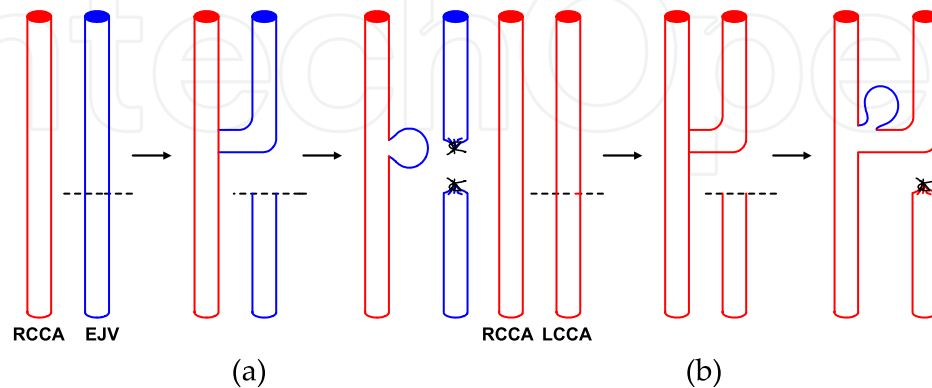
3.3.1. Surgical models

The technique used in the surgical construction of experimental aneurysm is based on grafting a venous pouch (usually taken from the external jugular vein) onto the common carotid artery. The main advantage of this approach is that the constructed aneurysms exhibit hemodynamic features that are very similar to those of humans. the disadvantages of constructed aneurysms include their venous histology and resistance to rupture.

With regard to the construction site, the graft might be placed on the lateral wall or at bifurcations. There are five main techniques to construct lateral wall aneurysms:

1. Non-ligated venous pouch with end-to-side anastomosis to the artery.
2. Non-ligated venous pouch with side-to-side anastomosis to the artery (variation of the former).
3. End-to-side anastomosis of the vein onto the artery with ligated venous pouch.
4. Side-to-side anastomosis of the vein onto the artery with ligated venous pouch.
5. End-to-side anastomosis of the venous pouch. The main advantage of this technique is the short-lasting clamping of the common carotid artery that thus avoids endothelial damage and vasospasm[21].

The main model for the construction of bifurcation aneurysms was performed using Forrest and O'Rielly's technique, in which the left common carotid artery of rabbits was partially anastomosed with the right common carotid artery. Next, a venous pouch (taken from the external jugular, anterior facial, or posterior facial vein) was grafted onto the knot formed by the union of the arterial anastomoses. The advantage of this technique was that unlike the lateral wall aneurysms, it did not induce aneurysmal thrombosis (**figure 3**)[24].

Figure 3. Graphic representation of the main surgical models of experimental saccular aneurysm. (a) Lateral wall, (b) bifurcation (RCCA – right common carotid artery, EJV – external jugular vein, LCCA – left common carotid artery).

3.3.2. Other experimental models of aneurysms

In addition to the abovementioned techniques, other methods have been attempted to construct saccular aneurysms, such as hyper-flow (through the creation of arteriovenous fistulas), trauma (traumatic puncture of the arterial wall or using CO_2 laser), and chemical wall injury (by injecting nitrogen mustard or other substances directly inside the arterial wall) [51]. All of these techniques are less efficient than chemical induction and surgical construction. Despite these attempts at the construction of an experimental model of saccular aneurysm, none of these methods was able to reproduce all of the histopathological, geometric, and hemodynamic features of human intracranial saccular aneurysms [51-54]. Nevertheless, the enzymatic method has stood out in recent years.

3.3.3. Enzymatic models

3.3.3.1. Elastase-induced model

3.3.3.1.1. Mechanisms of action of elastase in aneurysm formation

The formation of saccular aneurysms depends on several mechanisms, including inflammatory reaction, weakening of the arterial wall, and hemodynamic tension. Enzymatic imbalance and inflammatory activity are some of the potential causes involved in aneurysm formation in humans. Anidjar (1992) perfused the abdominal aorta of a group of Wistar rats with pancreatic elastase from swine and used thioglycollate plus plasmin (activators of the inflammatory response) in another group of animals. Both groups exhibited an inflammatory reaction, elastic lamina fragmentation, and formation of fusiform aneurysms similar to those

that occur in humans. The inflammatory activity was stronger in the elastase group (achieving its peak on the sixth day) and produced macrophages, polymorphonuclear cells, helper and suppressor T lymphocytes in the arterial wall. Combined with the progression of the inflammatory activity, the diameter of the abdominal aorta increased[55]. Halpern (1994) established the sequence and synchrony of induction of the inflammatory response. Elastase induces injury of the arterial wall, which triggers an initial inflammatory response. The inflammatory cells then activate endogenous proteinases (molecular weight between 50 and 90 kD) and the destruction of elastin and collagen, in addition to aortic dilation. Halpern's study showed that the rupture of elastin and its contact with macrophages are the main events in the activation of endogenous proteinases, which results in increased tissue destruction [56].

Although inflammatory activity might lead to destruction of the elastic fibers and a weakening of the arterial wall, its role in the development of saccular aneurysms has not been fully established. Other mechanisms may also participate in aneurysm formation such as alterations of the mechanical properties of arteries together with the hemodynamic tension on the vascular wall, which can produce aneurysms by themselves. Miskolczi (1997) demonstrated this phenomenon in an in vitro study, in which the common carotid arteries of swine and sheep were isolated and their walls were digested using pancreatic elastase from swine. Next, the arterial segments were placed between a pulsatile flow artificial pump and a series of test tubes, which allowed the control of variables such as flow, pulsation, and pressure without inducing the inflammatory response that occurs in in vivo studies. Consequently, small saccular aneurysms appeared at the sites where the elastin was damaged and hemodynamic tension was exerted on the weakened arterial wall[57].
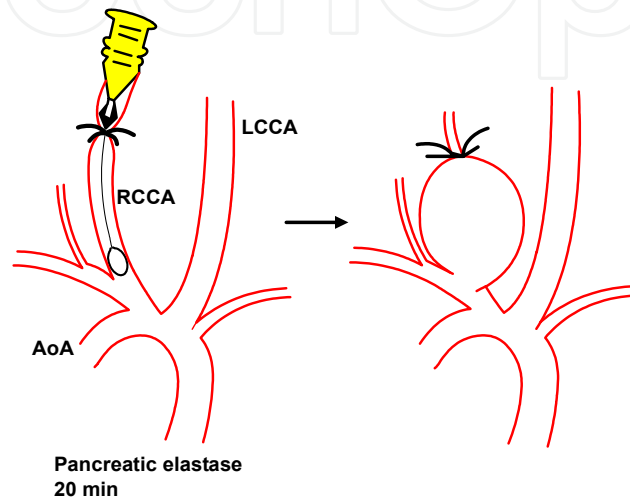
3.3.3.1.2. Creation and improvement of the elastase-induced model

Based on studies of experimental aneurysm creation using elastase [55, 56], Cawley et al. (1996) developed a new experimental model of lateral wall aneurysms in rabbits. This model consisted of dissecting the neck of rabbits, ligating the proximal segment of the external carotid artery, and performing intra-arterial perfusion of pancreatic elastase from swine. Three weeks later, saccular aneurysms were formed, which, from angiographic and histological perspectives, were very similar to those in humans. However, the lumen remained patent in only 40% of the aneurysms, because lateral aneurysms do not originate from the type of hemodynamic stress and intra-aneurysmal blood flow that occur at the bifurcations of the human cerebral arteries[58].

Cloft et al. (1999) improved this model by producing greater hemodynamic stress on the left common carotid artery (LCCA), which was directly hit by the blood flow from the ascending aorta in two-thirds of the rabbits. This technique is fully endovascular and consists of insufflating a balloon at the origin of the LCCA and isolating a small arterial segment for intraluminal infusion of bovine pancreatic elastase for 30 minutes. Angiographic control was performed by the dissection and retrograde puncture of the femoral arteries. This method succeeded in producing aneurysms with an average size of 3.0 mm x 5.0 mm whose lumen remained patent up to three months after creation. From a microscopic point of view, all of the aneurysms exhibited intact endothelium, the absence of an inflammatory response, moderately damaged elastic lamina inside of the aneurysm (but undamaged at the neck), and

apical thrombus. No animal exhibited neurological sequelae (due to the intracranial collateral vessels network) or showed systemic signs of elastase intoxication[59].

Kallmes et al. (1999) modified this method by creating additional hemodynamic tension on the proximal segment of the right common carotid artery (RCCA), which is located between the brachiocephalic artery and ascending aorta, and mimics a "bifurcation aneurysm." In addition, the long curvature of the brachiocephalic artery increased the hemodynamic tension at the origin of the RCCA compared to the LCCA. Further modification of this model consisted of reducing the time of enzymatic digestion to 20 minutes (**figure 4**).

LCCA

RCCA

AoA

Pancreatic elastase
20 min

Figure 4. Graphic representation of the endovascular elastase-induced aneurysm construction technique. AoA – aortic arch, RCCA – right common carotid artery and LCCA – left common carotid artery. Modified from Hoh, 2004[60].

These technical modifications resulted in experimental aneurysms similar to those observed in humans with regard to the arterial origin, shape, hemodynamics, and patency. The high hemodynamic tension caused by the long curvature of the brachiocephalic artery makes these experimental aneurysms similar to those occurring in the ophthalmic segment of the human internal carotid artery[40]. Altes et al. (2000) used the RCCA for the intraluminal infusion of pancreatic elastase from swine in rabbits and obtained aneurysms in 89% of the animals. Two weeks later, the elastic lamina ruptured and aneurysms were formed (average dimensions of 4.5 mm x 7.5 mm), with organized thrombus in the aneurysm dome, whereas the elastic lamina was undamaged in the walls of the parent arteries. The cells present in the organized thrombus exhibited features of smooth muscle cells and fibroblasts. Ten weeks later, no significant alterations were observed. The execution of this technique required less than one hour, and although it included surgical procedures (e.g., section of the RCCA), this technique exhibited lower morbidity and mortality compared to the use of the LCCA[43].

From a technical perspective, it is noteworthy that the concentration of elastase and the time of incubation exert a partial effect on the size of the aneurysms. One study compared animals that were not subjected to elastase to animals that were subjected to low, medium, and high concentrations of this drug, under variable durations. The rabbits that were not subjected to elastase exhibited complete thrombosis of the arterial stump and did not form

aneurysms, whereas the rabbits that were given elastase in progressive concentrations formed aneurysms. The increase of the elastase dose above a given value did not influence the size of the aneurysms; however, high concentrations of elastase induced the dilation of the parent artery and resulted in a more complex geometry of the aneurysm neck, which is closer to that observed in human aneurysms. Low concentration (25%) of elastase induced aneurysms without dilation of the adjacent artery[61].

Hoh et al. (2004) developed a simpler technique of construction and obtained aneurysms similar to those previously mentioned. The first simplification consisted of the use of a 24-gauge angiocatheter (instead of an introducer) and transitory occlusion of the origin of the RCCA using a neurosurgical clamp (instead of a balloon)[60]. The second simplification was achieved using an accurate neurological assessment of the rabbits using a four-point scale to rate the observed movements of the rabbits on a flat surface to verify whether paresis of the legs or abnormal gait occurred (movements in a circle or difficulty to walk). Accordingly, the animals were rated as grade I – no neurological deficit; grade II: minimal of suspected neurological deficit; grade III: mild neurological deficit without abnormal motion; and grade IV: remarkable neurological deficit and abnormal motion[62].

Although the studies performed to date have not reported any loss of animals, Möller-Hartmann et al. (2003) found a mortality of 25% due to the accidental passage of elastase into the superior thyroid artery with an aberrant origin or into the tracheoesophageal branch, which originated in the common carotid artery, resulting in hemorrhagic necrosis of the trachea[63]. Another source of undesirable distribution of elastase and tracheal necrosis is the anomalous origin of the tracheobronchial artery, which can be identified in angiographies as a small branch perpendicular to the proximal part of the RCCA, and runs medially towards the trachea[64]. Therefore, the elimination of those anomalous vessels (by ligation, coagulation or placing of the introducer lower inside the RCCA) is crucial for success in aneurysm creation by intraluminal infusion of elastase[63].

In addition to the problem posed by aberrant vessels, Krings et al. (2003) identified two additional potential causes of failure of the elastase model. The first potential cause depends on how elastase is injected through the introducer. Thus, instead of elastase, the blood column of the introducer dead space is pushed into the arterial lumen. Furthermore, the authors observed that doses of 100U of elastase were usually lethal. To address these problems, the authors reduced the dose of elastase to 20 U and performed a contrast injection test to detect aberrant arteries as follows: after occluding with a balloon in the proximal area of the RCCA, a non-ionic contrast material was injected (by means of an introducer) inside the RCCA, and the contrast column was verified for two minutes. If the contrast material remained, without washing out or dilution for two minutes, the test was deemed to be negative, i.e., there were no anomalous vessels. Otherwise, the test was deemed to be positive, and the introducer was advanced to a more proximal site of the RCCA where the contrast washing out or dilution no longer occurred. When these procedures were applied, none of the animals died, and all developed aneurysms. The full duration of this procedure was 40 minutes. The problem posed by the blood column and contrast material inside of the introducer was resolved by performing continuous suction using a syringe[65].

Prospective studies on the morphology and viability of elastase-induced aneurysms in rabbits require serial high-quality angiographic control. Three routes are currently used: the femoral arteries, left external auricular vein, and left central auricular artery. Miskolczi et al. (2005) suggested performing a retrograde puncture of the left central auricular artery as the best route, because the femoral artery is narrow and fragile and thus exhibits a high risk of injury and definitive loss. In addition, retrograde femoral catheterization requires the dissection of the groin, arteriotomy, and subsequent ligation with permanent vascular occlusion, thus making subsequent angiography at this site impossible. Puncture of the left external auricular vein allows for repeated injections of contrast material, but the resulting images exhibit low spatial resolution and frequent motion-related artifacts. In contrast, the left central auricular artery allows for repeated injections, high-quality images, and excellent visualization of the brachiocephalic trunk vessels because rabbits usually exhibit LCCA of bovine origin; thus, when the contrast material is injected into the left central auricular artery, the brachiocephalic trunk and its branches immediately become filled. When the LCCA originates directly from the aortic arch or from a common origin with the brachiocephalic trunk, but the angle is unfavorable, the contrast material only fills the distal aortic arch. The anatomy of approximately 70% - 80% of white New Zealand rabbits is favorable for retrograde injection in the left central auricular artery; therefore, pre-selection is important to exclude animals with unfavorable anatomy from studies[66].

3.3.3.1.3. Morphological and geometric features

The elastase model efficiently reproduces aneurysms similar to ones that occur in the ophthalmic segment of the human internal carotid artery with regard to width, height, neck size, and diameter of the parent artery. These characteristics were very well established by Short et al. (2001), who prospectively studied 40 rabbits and observed that the size of the aneurysmal cavities afforded by the elastase model was appropriate for preclinical tests of endovascular occlusion techniques and devices. The authors measured the width (points in the cavity exhibiting the maximal width), height (measurement of the aneurysmal dome to the mid-portion of a line connecting the proximal and distal portions of the aneurysm neck), neck (maximal diameter between the proximal and distal portions of the aneurysm orifice), the diameter of the parent artery (diameter of the artery just proximal to the aneurysm neck), and the dome/neck ratio (maximal dome width/neck width). In addition, they classified the aneurysms as small (2.0 mm – 4.9 mm), medium-sized (5.0 mm – 9.9 mm), or large (10.0 – 16.0 mm). Moreover, the neck was classified as small (< 4 mm) or wide (> 4 mm). Two weeks later, all of the animals had survived, none showed clinical evidences of neurological insult, and exhibited aneurysms at the apex of the long curve of the brachiocephalic artery, with an elongated shape, and a height greater than the width. Medium-sized (50%) and large (42.5%) aneurysms with small necks (55%) prevailed. The average width of the cavity was 4.1 ± 1.2 mm, which varied between 2.5 and 7.1 mm, and the average height was 8.8 ± 2.6 mm, which varied between 3.0 and 15.6 mm. A dome/neck ratio > 1 was observed in 50% of the aneurysms with an average value of 1.13 ± 0.5, and the average diameter of the parent artery was 4.3 ± 1.4 mm. Although these measures were similar to those of human aneurysms, they did not reproduce all of the corresponding morphological characteristics, which are difficult to quantify for many reasons[44].

Short-term follow-up of elastase-induced aneurysms showed that their dimensions increased gradually up to the end of the first month after creation and then become stable. The average measurements of the dome width and length at days 3 and 28 after induction were (3.2 ± 0.6 mm; 5.0 ± 0.9 mm) and (6.0 ± 1.3 mm; 10.0 ± 2.2 mm), respectively. Conversely, the aneurysms that were not incubated with elastase progressively retracted and formed thrombi inside. Because a millimeter-scale was used and the differences found were small, the authors considered the low resolution of intravascular angiography, radiographic projections used, and variations of the cardiac cycle that promoted different intra-aneurysmal pressures to be potential sources of variation and the lack of histological correlation to be a limitation of the study[67]. Ding et al. (2006) studied the long-term permeability of elastase-induced aneurysms and observed that the aneurysmal cavity remained patent and without thrombi for up to two years after creation and that after the first month, their dimensions (width, height, and neck width) did not exhibit significant variation [68].

The size of the neck has paramount importance when testing endovascular devices, as well as in the study of the physiopathology of aneurysms, and might be modified during the construction of experimental aneurysms. This finding was revealed by Ding et al. (2005), who observed that the size of the neck might be controlled by adjusting the position of the balloon during incubation with elastase. When the balloon is placed high, that is, half inside the proximal RCCA and half inside the subclavian and brachiocephalic arteries, the neck of the resulting aneurysms is narrow (< 4 mm). When the balloon is placed low, that is, exclusively inside of the subclavian and brachiocephalic arteries, the neck of the resulting aneurysms is wide (> 4 mm). The authors further observed that the position of the balloon did not influence the length of the aneurysms and that the balloons that were placed low did not always result in wide necks[69].

In addition to the low position of the balloon, the geometric relationship between the longest axis of the aneurysms and the axis of the parent artery played an important role in the determination of local hemodynamics and the final architecture of aneurysms. Onizuka et al. (2006) compared the angle formed by the longest axis of aneurysms and the axis of the parent artery immediately and three months after aneurysm construction. The authors found a positive correlation between the neck size and the dome height. In addition, the dome height was proportional to the angle formed by the brachiocephalic artery and the aneurysm neck. Therefore, the authors concluded that the larger the angle, the greater the hemodynamic stress caused by the blood flow on the distal neck and the aneurysm bottom[70].

The volume of elastase-induced aneurysms might also be adjusted by the position of the RCCA ligation so that high ligations might create relatively larger aneurysms compared to the ones produced by low ligations. Ding et al. (2007) prospectively studied the influence of the height of the RCCA ligation on the volume of aneurysms. Ligations were rated lower when the height of the ligation point was 10-mm away from the origin of the RCCA and high when the ligation point was 15-mm away from the origin of the RCCA. The same authors applied the formula for the volume of cylinders to calculate the volume of aneurysms because the shape of the created aneurysms was cylindrical. The aneurysms with higher ligations exhibited larger volumes (102.4 ± 54.8 mm^3) compared to the ones with lower ligations (36.6 ± 26.8 mm^3). In addition, the aneurysms with higher ligations exhibited

larger dimensions such as the neck (3.3 ± 0.8 mm), width (3.7 ± 0.7 mm), and height (9.0 ± 1.7 mm). The authors attributed these results to a larger cavity space of aneurysms with higher ligation, in addition to probable greater hemodynamic stress on the aneurysms. Finally, according to those authors, no animals died due to the accidental passage of elastase (through aberrant vessels) in the case of aneurysms with higher ligation[69].

3.3.3.1.4. Histology

Abruzzo et al. (1998) compared the histological characteristics between lateral wall aneurysms (produced by means of elastase incubation in the external carotid artery of rabbits) and lateral wall aneurysms constructed by grafting a venous pouch onto the common carotid artery of pigs. Both experimental aneurysms were compared to human aneurysms with 5 – 10 mm of diameter (recently ruptured and obtained at autopsy), whose main characteristics included: 1) a complete absence of the internal elastic lamina in the aneurysms, and abrupt termination of the internal elastic lamina of the parent artery at the margins of the saccular orifice; 2) complete absence of the tunica media in the aneurysms and abrupt termination of the tunica media of the parent artery at the margins of the aneurysmal orifice; 3) absence of intramural inflammatory reaction in the aneurysms; 4) absence of neointimal fibromuscular proliferation; 5) a sac wall thickness of 51 μm and a neck thickness of 52 μm. In three out of the five studied aneurysms, one-third of the aneurysmal cavity was filled by a thrombus at different stages of organization and firmly adhered to the point of rupture. The elastase-induced aneurysms exhibited an abrupt termination of the internal elastic lamina at the margins of the saccular orifice, but the tunica medica was undamaged and continued into the interior of the saccular part of the aneurysms. The sac walls exhibited a mild to moderately inflammatory cellular (monocytes and neutrophils) response and a mild fibromuscular response. The thickness of the neck was 49 μm, and the thickness at the sac wall was 44 μm. An unorganized thrombus filled one-third of the aneurysmal cavity in two out of the four investigated rabbits. The aneurysms constructed using a venous pouch exhibited a well-developed elastic lamina, and the tunica media extended into the sac wall. The wall of the venous pouch contained remarkable inflammatory infiltrate (monocytes and neutrophils) and extreme degrees of fibromuscular proliferation completely across the aneurysm wall, resulting in a remarkable neointimal thickening and luminal narrowing. The thickness of the dome wall was 228 μm, and the thickness at the neck was 350 μm. Thus, the authors concluded that from a histological perspective, the elastase-induced aneurysms were the ones most similar to human aneurysms, in addition to exhibiting little spontaneous fibromuscular response compared to the surgical model with venous pouch grafting[71]. Accordingly, the elastase-induced model is currently used in tests for endovascular devices[39-42].

3.3.3.2. Papain-induced model

Although the damage of elastic fibers induced by swine pancreatic elastase resulted in experimental aneurysms similar to those appearing in the ophthalmic segment of the human internal carotid artery, they are small (<5 mm), which is not completely consistent with the actual clinical characteristics of human aneurysms, where the aneurysms are larger than 5 mm. To overcome this limitation, Chinese researchers tested an association between elastase and collagenase in the *in vitro* pre-digestion of an arterial pouch grafted onto the aortic arch

of rabbits; however, that model exhibited a higher tendency to spontaneously rupture[72]. To produce saccular aneurysms larger than 5 mm, De Oliveira et al. (2011) infused the papain enzyme successfully inside the right common carotid artery of rabbits[73].

3.3.3.3. Mechanisms of action of papain

Papain is a cysteine-proteinase type of endolytic enzyme extracted from the latex of green papaya (*Carica papaya*). It weighs 23,000 Da , and its molecules form a single peptide chain with 211 amino acid residues that fold into two distinct parts, which are divided by a cleft that represents its active site[74]. In addition to papain, the latex contains three additional enzymes (chymopapain, caricain, and glycil endopeptidase), which together with papain represent 80% of the enzymatic fraction, where papain corresponds to the smallest enzymatic fraction (5-8%). Although purification of papain is usually performed using precipitation techniques, it remains contaminated by other proteases[75]. With regard to its enzymatic activity, papain is activated by the addition of substances such as cyanide, reduced glutathione, and sulfate and is inactivated by oxidants. The maximal enzymatic activity occurs with a pH between 5 and 7.5. With regard to its specificity, in addition to hydrolyzing several substances, papain exhibits strong esterase activity, which makes its scope of action even wider to the point of acting on the very same substrates as pancreatic proteolytic enzymes with esterase activity[76].

Regarding its biological effects, papain exhibits remarkable elastolytic properties and has been successfully used in the production of experimental lung emphysema in animals[77, 78]. In addition to digesting elastic fibers, papain is also able to destroy collagen. Junqueira (1980) studied the ability of papain to destroy the collagen fibers of several tissues (cartilage, bone, skin, and blood vessel) from several animal species, such as *Gallus gallus* (chicken), *Canis familiaris* (dog), *Oryctolagus cuniculus* (rabbit) and *Sus scrofa* (pig), and observed that the degree of collagen destruction varies according to the type of tissue[79]. Ionescu (1977) used papain to de-antigenize a venous heterograft to subsequently graft it onto the common carotid artery of dogs and observed that papain caused an excessive weakening of the graft with a tendency to form venous aneurysms. To overcome this problem, the author subjected the grafts to a previous treatment with formol to maintain their rigidity and flexibility and not form aneurysms[80].

With regard to commercial presentation, papain is found as raw latex (~ 12 U/mg), lyophilized powder (10 U/mg) and aqueous suspension (16-40 U/mg)[81].

3.3.3.4. Creation of papain-induced aneurysms

The technique applied in the construction of papain-induced aneurysms uses the right common carotid artery of rabbits and is fully surgical, based on the study by Hoh et al. However, this technique does not use angiography during the puncture of the right common carotid artery and injection of the enzyme. This simplification proved to be safe and efficacious, and no animal exhibited complications due to the unduly passage of papain to an aberrant vascular branch that was accidentally present in the neck of the animals. Other innovations were the removal of the aortic arch and the supra-aortic trunks, direct measurement of the macroscopic dimensions of aneurysms and vessels using a caliper, and

quantitative histological studies by means of histomorphometry in addition to a qualitative histological analysis[60,73].

3.3.3.5. Morphologic and geometric features

Papain-induced aneurysms exhibited a size similar to the elastase-induced aneurysms described in previous studies. Nevertheless, it is noteworthy to stress that the papain-induced aneurysms were measured directly on the right common carotid artery. This is an important point because most of the studies performed using elastase employed digital subtraction angiography to measure the aneurysms, which led to an overestimate of the aneurysm size. Thus, if papain-induced aneurysms were also measured by means of digital subtraction angiography, then their size would have most likely been overestimated. Independent from the method used, papain was efficacious in producing saccular aneurysms with an average diameter of 3.8 +/- 1.4 mm (2.5-7.0 mm), similar to those appearing in the ophthalmic segment of the human internal carotid artery.

3.3.3.6. Histology

From a histological perspective, papain caused the destruction of elastic fibers, endothelial damage, thrombosis, and intimal fibrosis. These alterations are similar to those found in elastase-induced aneurysms, in which the only difference is the degree of thrombosis, which was more remarkable in the papain-induced aneurysms[73].

3.3.3.7. Future of the enzymatic model

Currently, there are no ideal animal models of experimental saccular aneurysms available. From a practical perspective, it is impossible for one single model to reproduce the full histological, geometric, and hemodynamic characteristics of the wide variety of aneurysms and human-related conditions. Nevertheless, the enzymatic model has been increasingly used in the production of saccular aneurysms due to its simplicity, easy execution, and lower cost, resulting from the use of small animals such as rabbits, in addition to allowing the control of height, width, and size of the aneurysm neck. Furthermore, the enzymatic model can be improved, as a wide variety of enzymes have not yet been tested. Despite the advantages of the enzymatic model, the use of both elastase and papain exhibits some limitations, such as an intramural inflammatory response, endothelial damage, and thrombosis. Indeed, thrombosis is the most important effect because it hinders the interpretation of the results of the embolization materials tested. However, even when they are present, the intra-aneurysmal thrombi do not invalidate this experimental model because under actual clinical conditions, most human aneurysms have thrombi present. Therefore, although they are not ideal for preclinical tests of embolization materials, enzymatic models most closely mimic the actual clinical conditions and thus exhibit a high potential to contribute to the study of the physiopathology of human intracranial aneurysms and testing of embolization materials and endovascular devices.

Author details

Ivanilson Alves de Oliveira
Neuroradiology, Experimental Medicine Laboratory, Universidade Federal de Sergipe-UFS, Brazil

4. References

[1] Nyström H.S.M. Development of intracranial aneurysms as revealed by electron microscopy. J Neurosurg, 1963. 20: p. 329-337.

[2] Rhoton A.L., Jr. Anatomy of saccular aneurysms. Surg Neurol, 1980. 14(1): p. 59-66.

[3] Senegor M. Traumatic pericallosal aneurysm in a patient with no major trauma. Case report. J Neurosurg, 1991. 75(3): p. 475-7.

[4] Barker C.S. Peripheral cerebral aneurysm associated with a glioma. Neuroradiology, 1992. 34(1): p. 30-2.

[5] Frazee J.G., Cahan L.D. and Winter J. Bacterial intracranial aneurysms. J Neurosurg, 1980. 53(5): p. 633-41.

[6] Lee K.S., Liu S.S., Spetzler R.F., Rekate H.L. Intracranial mycotic aneurysm in an infant: report of a case. Neurosurgery, 1990. 26(1): p. 129-33.

[7] Bohmfalk G.L., Story J.L., Wissinger J.P., Brown, W.E. Bacterial intracranial aneurysm. J Neurosurg, 1978. 48(3): p. 369-82.

[8] Brown R.D., Jr., Wiebers D.O. and Forbes G.S. Unruptured intracranial aneurysms and arteriovenous malformations: frequency of intracranial hemorrhage and relationship of lesions. J Neurosurg, 1990. 73(6): p. 859-63.

[9] Brown B.M. and Soldevilla F. MR angiography and surgery for unruptured familial intracranial aneurysms in persons with a family history of cerebral aneurysms. AJR Am J Roentgenol, 1999. 173(1): p. 133-8.

[10] Schievink W.I., Parisi J.E, Piepgras D.G., Michels V.V. Intracranial aneurysms in Marfan's syndrome: an autopsy study. Neurosurgery, 1997. 41(4): p. 866-70; discussion 871.

[11] Heiserman J.E., Drayer B.P., Fram E.K., Keller P.J. MR angiography of cervical fibromuscular dysplasia. AJNR Am J Neuroradiol, 1992. 13(5): p. 1454-7.

[12] Kopitnik T.A. and Samson D.S. Management of subarachnoid haemorrhage. J Neurol Neurosurg Psychiatry, 1993. 56(9): p. 947-59.

[13] Dix G.A., Gordon W., Kaufmann A.M., Sutherland I.A., Sutherland G.R. Ruptured and unruptured intracranial aneurysms--surgical outcome. Can J Neurol Sci, 1995. 22(3): p. 187-91.

[14] Winn H.R., Almaani W.S., Berga S.L., Jane J.A., Richardson A.E. The long-term outcome in patients with multiple aneurysms. Incidence of late hemorrhage and implications for treatment of incidental aneurysms. J Neurosurg, 1983. 59(4): p. 642-51.

[15] Yasargil M.G. and Fox J.L. The microsurgical approach to intracranial aneurysms. Surg Neurol, 1975. 3(1): p. 7-14.

[16] Guglielmi G., Vinuela F., Dion J., Duckwiler G. Electrothrombosis of saccular aneurysms via endovascular approach. Part 2: Preliminary clinical experience. J Neurosurg, 1991. 75(1): p. 8-14.

[17] Derdeyn C.P., Barr J.D., Berenstein A., Connors J.J., Dion J.E., Duckwiler G.R., Higashida R.T., Strother C.M., Tomsick T.A., Turski P. The International Subarachnoid Aneurysm Trial (ISAT): a position statement from the Executive Committee of the American Society of Interventional and Therapeutic Neuroradiology and the American Society of Neuroradiology. AJNR Am J Neuroradiol, 2003. 24(7): p. 1404-8.

[18] Fagundes D.J., Taha M.O. Modelo animal de doença:critérios de escolha e espécies de animais de uso corrente. Acta Cirúrgica Brasileira, 2004. 19(1): p. 59-65.

[19] Hashimoto N., Handa H. and Hazama F. Experimentally induced cerebral aneurysms in rats. Surg Neurol, 1978. 10(1): p. 3-8.

[20] German W.J. and Black S.P.W. Experimental production of carotid aneurysms. N Engl J Med, 1954. 250(3): p. 104-6.

[21] Massoud T.F., Guglielmi G., Ji C., Vinuela F., Duckwiler G.R. Experimental saccular aneurysms. I. Review of surgically-constructed models and their laboratory applications. Neuroradiology, 1994. 36(7): p. 537-46.

[22] Schanaider A., Silva P.C., The use of animals in experimental surgery. Acta Cirúrgica Brasileira, 2004. 19(4): p. 1-9.

[23] Hashimoto N., Kim C., Kikuchi H., Kojima M., Kang Y., Hazama F. Experimental induction of cerebral aneurysms in monkeys. J Neurosurg, 1987. 67(6): p. 903-5.

[24] Forrest M.D. and O'Reilly G.V. Production of experimental aneurysms at a surgically created arterial bifurcation. AJNR Am J Neuroradiol, 1989. 10(2): p. 400-2.

[25] Hashimoto N., Handa H. and Hazama F. Experimentally induced cerebral aneurysms in rats: part II. Surg Neurol, 1979. 11(3): p. 243-6.

[26] Hashimoto N., Handa H. and Hazama F. Experimentally induced cerebral aneurysms in rats: Part III. Pathology. Surg Neurol, 1979. 11(4): p. 299-304.

[27] Kerber C.W. and Buschman R.W. Experimental carotid aneurysms: I. Simple surgical production and radiographic evaluation. Invest Radiol, 1977. 12(2): p. 154-7.

[28] Nagata I., Handa H. and Hashimoto N. Experimentally induced cerebral aneurysms in rats: part IV--cerebral angiography. Surg Neurol, 1979. 12(5): p. 419-24.

[29] Hashimoto N., Handa H. Nagata I., Hazama, F. Experimentally induced cerebral aneurysms in rats: Part V. Relation of hemodynamics in the circle of Willis to formation of aneurysms. Surg Neurol, 1980. 13(1): p. 41-5.

[30] Nagata I., Handa H., Hashimoto N., Hazama F. Experimentally induced cerebral aneurysms in rats: Part VI. Hypertension. Surg Neurol, 1980. 14(6): p. 477-9.

[31] Nakatani H., Hashimoto N., Kikuchi H., Yamaguchi S., Niimi H. In vivo flow visualization of induced saccular cerebral aneurysms in rats. Acta Neurochir (Wien), 1993. 122(3-4): p. 244-9.

[32] Stehbens W.E. Experimental production of aneurysms by microvascular surgery in rabbits. Vasc Surg, 1973. 7(3): p. 165-75.

[33] de los Reyes R.A., Boehm F.H., Boehm F.H., Ehler W., Kennedy D., Shagets F., Woodruff W., Smith T. Direct angioplasty of the basilar artery in baboons. Surg Neurol, 1990. 33(3): p. 185-91.

[34] Yoshino Y., Niimi Y., Song J.K., Khoyama S., Shin Y.S., Berenstein A. Endovascular treatment of intracranial aneurysms: comparative evaluation in a terminal bifurcation aneurysm model in dogs. J Neurosurg, 2004. 101(6): p. 996-1003.

[35] Graves V.B., Strother C.M., Partington C.R., Rappe A. Flow dynamics of lateral carotid artery aneurysms and their effects on coils and balloons: an experimental study in dogs. AJNR Am J Neuroradiol, 1992. 13(1): p. 189-96.

[36] Spetzger U., Reul J., Weis J., Bertalanffy H., Thron A., Gilsbach J.M. Microsurgically produced bifurcation aneurysms in a rabbit model for endovascular coil embolization. J Neurosurg, 1996. 85(3): p. 488-95.

[37] Spetzger U., Reul J., Weis J., Bertalanffy H., Gilsbach J.M. Endovascular coil embolization of microsurgically produced experimental bifurcation aneurysms in rabbits. Surg Neurol, 1998. 49(5): p. 491-4.

[38] Raymond J., Salazkin I., Metcalfe A., Robledo O., Gevry G., Roy D., Weill A., Guilbert F. Lingual artery bifurcation aneurysms for training and evaluation of neurovascular devices. AJNR Am J Neuroradiol, 2004. 25(8): p. 1387-90.

[39] Kallmes D.F., Helms G.A., Hudson S.B., Altes T.A., Do H.M., Mandell J.W., Cloft H.J. Histologic evaluation of platinum coil embolization in an aneurysm model in rabbits. Radiology, 1999. 213(1): p. 217-22.

[40] Kallmes D.F., Williams A.D., Cloft H.J., Lopes M.B., Hankins G.R., Helm G.A. Platinum coil-mediated implantation of growth factor-secreting endovascular tissue grafts: an in vivo study. Radiology, 1998. 207(2): p. 519-23.

[41] Hans F.J., Krings T., Möller-Hartmann W., Thiex R., Pfeffer J., Cherer K., Brunn A., Dreeskamp H., Stein K.P., Meetz A., Gilsbach J.M., Thron A. Endovascular treatment of experimentally induced aneurysms in rabbits using stents: a feasibility study. Neuroradiology, 2003. 45(7): p. 430-4.

[42] Struffert T., Roth C., Romeike B., Grunwald I.O., Reith W. Onyx in an experimental aneurysm model: histological and angiographic results. J Neurosurg, 2008. 109(1): p. 77-82.

[43] Altes T.A., Cloft H.J., Short J.G., DeGast A., Do H.M., Helm G.A., Kallmes D.F. 1999 ARRS Executive Council Award. Creation of saccular aneurysms in the rabbit: a model suitable for testing endovascular devices. American Roentgen Ray Society. AJR Am J Roentgenol, 2000. 174(2): p. 349-54.

[44] Short J.G., Fujiwara N.H., Marx W.F., Helm G.A., Cloft H.J., Kallmes D.F. Elastase-induced saccular aneurysms in rabbits: comparison of geometric features with those of human aneurysms. JNR Am J Neuroradiol, 2001. 22(10): p. 1833-7.

[45] Adams D.F., Olin T.B. and Redman H.C. Catheterization of Arteries in the Rabbit. Radiology, 1965. 84: p. 531-5.

[46] Angel-James J. Variations in the vasculature of the aortic arch and its major branches in the rabbit. Acta Anat, 1974. 87: p. 283-300.

[47] Bugge J. Arterial supply of the cervical viscera in the rabbit. Acta Anat (Basel), 1967. 68(2): p. 216-27.

[48] Blanding J.D., Jr., Ogilvie R.W., Hoffman C.L., Knisely W.H. The Gross Morphology of the Arterial Supply to the Trachea, Primary Bronchi, and Esophagus of the Rabbit. Anat Rec, 1964. 148: p. 611-4.

[49] Du Boulay G.H. Comparative neuroradiologic vascular anatomy of experimental animals. In: Newton D.G. and Potts T.H. (ed.) Radiology of the skull and brain. Saint Louis: Mosby; 1974. p. 2763-86.

[50] Chungcharoen D., Daly M.B.; Neil E. The efect of occlusion upon the intrasinusal presure with special reference to vascular communications between the carotid and vertebral circulations in the dog, cat, and rabbit. J Physiol, 1952. 117: p. 56-76.

[51] Stehbens W.E. Evaluation of aneurysm models, particularly of the aorta and cerebral arteries. Exp Mol Pathol, 1999. 67(1): p. 1-14.

[52] Nishikawa M., Smith R.D. and Yonekawa Y. Experimental intracranial aneurysms. Surg Neurol, 1977. 7(4): p. 241-4.

[53] TerBrugge K.G., Lasjaunias P. and Hallacq P. Experimental models in interventional neuroradiology. AJNR Am J Neuroradiol, 1991. 12(6): p. 1029-33.

[54] Powell J. Models of arterial aneurysm: for the investigation of pathogenesis and pharmacotherapy--a review. Atherosclerosis, 1991. 87(2-3): p. 93-102.

[55] Anidjar S., Dobrin P.B., Eichorst M., Graham G.P., Chejfec G. Correlation of inflammatory infiltrate with the enlargement of experimental aortic aneurysms. J Vasc Surg, 1992. 16(2): p. 139-47.

[56] Halpern V.J., Nackman G.B., Gandhi R.H., Irizzary E., Scholes J.V., Ramey, W.G. The elastase infusion model of experimental aortic aneurysms: synchrony of induction of endogenous proteinases with matrix destruction and inflammatory cell response. J Vasc Surg, 1994. 20(1): p. 51-60.

[57] Miskolczi L., Guterman L.R., Flaherty J.D., Hpkins L.N. Saccular aneurysm induction by elastase digestion of the arterial wall: a new animal model. Neurosurgery, 1998. 43(3): p. 595-600; discussion 600-1.

[58] Cawley C.M., Dawson R.C., Shengelaia G., Bonner G., Barrow D.L., Colohan A.R. Arterial saccular aneurysm model in the rabbit. AJNR Am J Neuroradiol, 1996. 17(9): p. 1761-6.

[59] Cloft H.J., Altes T.A., MArx W.F., Raible R.J., Hudson S.B., Helm G.A., Mandell J.W. Jensen M.E., Dion J.E., Kallmes D.F., Endovascular creation of an in vivo bifurcation aneurysm model in rabbits. Radiology, 1999. 213(1): p. 223-8.

[60] Hoh B.L., Rabinov J.D., Pryor J.C., Ogilvy C.S. A modified technique for using elastase to create saccular aneurysms in animals that histologically and hemodynamically resemble aneurysms in human. Acta Neurochir (Wien), 2004. 146(7): p. 705-11.

[61] Kallmes D.F., Fujiwara N.H., Berr S.S., Helm G.A., Cloft H.J. Elastase-induced saccular aneurysms in rabbits: a dose-escalation study. AJNR Am J Neuroradiol, 2002. 23(2): p. 295-8.

[62] Endo S., Branson P.J. and Alksne J.F. Experimental model of symptomatic vasospasm in rabbits. Stroke, 1988. 19(11): p. 1420-5.

[63] Möller-Hartmann W., Krings T., Stein K.P., Dreeskamp A., Meetz A., Thiex R., Hans F.J., Gilsbach J.M., Thron A. Aberrant origin of the superior thyroid artery and the tracheoesophageal branch from the common carotid artery: a source of failure in elastase-induced aneurysms in rabbits. AJR Am J Roentgenol, 2003. 181(3): p. 739-41.

[64] Thiex R., Hans F.J., Krings T., Möller-Hartmann W., Brunn A., Scherer K., Gilsbach J.M., Thron A. Haemorrhagic tracheal necrosis as a lethal complication of an aneurysm model in rabbits via endoluminal incubation with elastase. Acta Neurochir (Wien), 2004. 146(3): p. 285-9; discussion 289.

[65] Krings T., Möller-Hartmann W., Hans F.J., Thiex R., Brunn A., Scherer K., Meetz A., Dreeskamp H., Stein K.P., Gilsbach J.M., Thron A. A refined method for creating saccular aneurysms in the rabbit. Neuroradiology, 2003. 45(7): p. 423-9.

[66] Miskolczi L., Nemes B., Cesar L., Masanari O. Gounis M. Contrast injection via the central artery of the left ear in rabbits: a new technique to simplify follow-up studies. AJNR Am J Neuroradiol, 2005. 26(8): p. 1964-6.

[67] Fujiwara N.H., Cloft H.J., Marx W.F., Short J.G., Jensen M.E., Kallmes D.F. Serial angiography in an elastase-induced aneurysm model in rabbits: evidence for progressive aneurysm enlargement after creation. AJNR Am J Neuroradiol, 2001. 22(4): p. 698-703.

[68] Ding Y.H., Dai D., Lewis D.A., Danielson M.A., Kadirvel R., Cloft H.J., Kallmes D.F. Long-term patency of elastase-induced aneurysm model in rabbits. AJNR Am J Neuroradiol, 2006. 27(1): p. 139-41.

[69] Ding Y.H., Dai D., Danielson M.A., Kadirvel R., Lewis D.A., Cloft H.J., Kallmes D.F. Control of aneurysm volume by adjusting the position of ligation during creation of elastase-induced aneurysms: a prospective study. AJNR Am J Neuroradiol, 2007. 28(5): p. 857-9.

[70] Onizuka M., Miskolczi L., Gounis M.J., Seong J., Lieber B.B., Wakhloo A.K. Elastase-induced aneurysms in rabbits: effect of postconstruction geometry on final size. AJNR Am J Neuroradiol, 2006. 27(5): p. 1129-31.

[71] Abruzzo T., Shengelaia G.G., Dawson R.C., Owens D.S., Cawley C.M., Gravanis M.B. Histologic and morphologic comparison of experimental aneurysms with human intracranial aneurysms. AJNR Am J Neuroradiol, 1998. 19(7): p. 1309-14.

[72] Yang X.J., Li L. and Wu Z.X. A novel arterial pouch model of saccular aneurysm by concomitant elastase and collagenase digestion. J Zhejiang Univ Sci B, 2007. 8(10): p. 697-703.

[73] de Oliveira I.A., Mendes Pereira Caldas J.G., Oliveira H.A., Brito E.A.C. Development of a new experimental model of saccular aneurysm by intra-arterial incubation of papain in rabbits. Neuroradiology, 2011. 53(11): p. 875-81.

[74] Drenth J., Jansonius J.N., Koekoek R., Swen H.M., Wolthers B.G. Structure of papain. Nature, 1968. 218(5145): p. 929-32.

[75] Nitsawang S., Hatti-Kaul R., Kanarawud P., Purification of papain from Carica papaya latex: aquous two-phase extraction versus two-step salt precipitation. Enzyme and Microbiolol technology., 2006: p. 1-5.

[76] Kimmel J.R., Smith E.L. Crystaline papain. I. Preparation,specificity and activation. J Biol Chem, 1954. 207(2): p. 515-531.

[77] Johanson W.G., Jr. and Pierce A.K. Effects of elastase, collagenase, and papain on structure and function of rat lungs in vitro. J Clin Invest, 1972. 51(2): p. 288-93.

[78] Gross P., Babyak M.A., Tolker E., Kaschak M. Enzymatically Produced Pulmonary Emphysema; a Preliminary Report. J Occup Med, 1964. 6: p. 481-4.

[79] Junqueira L.C., Bignolas G., Mourão P.A.S., Bonetti S.S., Quantitation of collagen - proteoglycan interaction in tissue sections. Connect Tissue Res, 1980. 7(2): p. 91-6.

[80] Ionescu G., Neumann E., Domokos M., Andercou A., Cardan E., Cucu A. Experimental preparation of deantigenized vascular heterografts and study of tolerance after transplantation. Acta Chir Belg, 1977. 76(4): p. 393-9.

[81] Sigma-Aldrich. Reagentes bioquímicos e kits para pesquisa em ciências da vida. Sigma-Aldrich (ed.); Brasil. 2006:p. 1812-1813.